Proceedings of the ASME 2011 Internal Combustion Engine Division Fall Technical Conference
ICEF2011
October 2-5, 2011, Morgantown, West Virginia, USA

ICEF2011-60076

KNOCK DETECTION AND CONTROL IN AN HCCI ENGINE USING DWT

Masoud Mashkournia*
Department of Mechanical Engineering
University of Alberta
Edmonton, Alberta T6G 2G8
Email: masoudm@ualberta.ca

Adrian Audet
Charles Robert Koch
Department or Mechanical Engineering
University of Alberta
Edmonton, Alberta T6G 2G8, Canada
Email: bob.koch@ualberta.ca

ABSTRACT

The novel application of the Discrete Wavelet Transform (DWT) in a real time controller is used to detect and subsequently control knock in a Homogeneous Charge Compression Ignition (HCCI) engine. Classical Fourier techniques for knock detection are discussed and compared to Wavelet Transforms. The Discrete Wavelet Transform filter bank is chosen as the best method for knock detection due to its good time-resolution and low computational requirements. The DWT method is compared with the root mean squared value of the pressure trace as the benchmark method for determining knock and the two methods are linearly correlated. Using the DWT method for knock detection and modulating fuel octane, both a Proportional Integral (PI) and PI with Feed-forward control are implemented. Both of these methods reduce knock intensity for a step increase in engine load. The combination of Feed-forward with PI feedback is found to be slightly more effective than just PI feedback control.

NOMENCLATURE

aBDC	After Bottom Dead Center
b	Cylinder bore
c	Speed of sound
CAD	Crank Angle Degrees
CWT	Continuous Wavelet Transform
DWT	Discrete Wavelet Transform
EGR	Exhaust Gas Recirculation
$f_{m,n}$	Expected knock frequency
F_{scaled}	Scaled frequency
F_{center}	Center frequency of a wavelet
FF	Feed-Forward
FF+PI	Feed-Forward with Proportional Integral
HCCI	Homogeneous Charge Compression Ignition
IVC	Intake Valve Closing
IVO	Intake Valve Opening
K_{PSD}	Knock index based on Power Spectral Density
m	Order of the circumferential mode
n	Order of the radial mode
N	Engine speed
ON	Octane Number
$\hat{p}$	Filtered pressure trace
P_{RMS}	Root mean squared of the Pressure trace
PI	Proportional Integral
PRF	Primary Reference Fuel
PSD	Power Spectral Density
RPM	Revolution Per Minute
s	Scale
SI	Spark Ignition
TDC	Top Dead Center
$\rho_{m,n}$	Oscillation mode factor
Δ	Sampling period
σ	Standard Deviation
κ	knock value

INTRODUCTION

As the price of fuel continues to rise and the emission standards for cars become more strict, it is increasingly important to develop more efficient methods of burning fossil fuels. Homogeneous Charge Compression Ignition (HCCI) combustion is a method where the fuel and air are pre-mixed and compressed in the combustion chamber until ignition occurs uniformly. This differs from spark ignition (SI) engines since there is no spark plug and differs from diesel since there is no direct injection event to time the combustion. Thus, in HCCI, combustion is

*Address all correspondence to this author.

timed by chemical kinetics and is difficult to control. This is compounded by the fact that there is limited time for air and fuel to mix creating a localized inhomogeneity. These localized inhomogeneities in either the local equivalence ratio, residual fraction, or temperature all slightly vary the local auto-ignition behavior of the mixture [1] [2] [3]. The global effect of these variations is that the ignition process begins in localized spots rapidly leading to auto-ignition over the entire combustion space [4]. Unbalanced pressures in the cylinder from the uneven combustion initiation results in oscillating pressure waves. As the mixture strength is increased, the potential for spatial variations in the mixture (compositional inhomogeneity in particular) grows, leading to larger pressure oscillations which manifest themselves as a sound similar to that of knock in an SI engine. The pressure oscillations in HCCI could conceivably give rise to engine damage similar to that experienced in SI engines due to engine knock or scrubbing of the thermal boundary layer present in the cylinder. Removing this boundary layer exposes the in-cylinder surfaces to the high temperature combustion gases, resulting in significantly increased heat transfer [5]. After the HCCI combustion, the descending piston as well as heat transfer cause the in-cylinder temperature to decrease. As the mixture temperature changes, the dominant resonance frequency of the pressure oscillations varies according to the local speed of sound of the mixture. The nature of knocking is thus a very transient one, as the rapid initiation of the oscillations during combustion is followed by a significant change in the characteristic frequency as the piston descends during the power stroke. One important difference between knock in HCCI and SI combustion, is that in HCCI, some level of pressure oscillations exist in virtually all engine conditions and in virtually all cycles. Where knock in SI results from the abnormal case of auto-ignition of the end gas zone, the pressure oscillations of HCCI are formed due to the normal auto-ignition of the in-cylinder mixture.

Numerous methods for detecting knock have been proposed. Typically, the pressure waves of knock resonate at a particular frequency that is characteristic of the combustion chamber geometry. So, the Fourier transform is often used to determine the presence of knock [6] [7]. However, for a non-stationary signal such as knock, traditional signal processing techniques are ill-suited as they rely on the assumption of a stationary, periodic signal. Furthermore as engine speeds increase additional mechanical noise from the valve train and piston movements reduce the SNR and greatly reduce the effectiveness of the traditional methods. The use of a wavelet transform to obtain time frequency resolution is advantageous for the transient HCCI knock [8]. Both continuous and discrete wavelet transforms have been used [9] [10] [4]. However, the continuous wavelet transform requires excessive computational effort [11] and so the computations are often done off-line. In order to be able to control the amount of knock in real-time on an engine, a more computationally efficient method is needed. The discrete wavelet transform is a promising method of knock detection.

Many knock control schemes have been proposed using a variety of knock detection methods. For spark ignition or diesel engines, actuators such as spark timing, exhaust gas recirculation or injection timing are used to influence the combustion and control of knock [12] [13] [14]. In HCCI, however, the most conventional actuation of spark timing or injection timing is not available. The use of multiple fuels is a growing area of research with promise [15] [16]. For HCCI combustion the high load operation is limited by knock [17]and can be reduced by increasing fuel octane number [15]. With this direct relationship known, the use of PRF as a controller can be explored. Thus in this study, the engine is operated near the knock limit, then the load is increased by increasing the amount of fuel injected. This causes engine knock which is detected and controlled by modulating fuel octane number.

ENGINE SETUP

Data for analysis was collected on a Ricardo Hydra Mark III single cylinder engine, fitted with a modified Mercedes E550 cylinder head. Basic engine geometry is in Table 1. The Mercedes series cylinder head represents a typical modern cylinder head with a pent-roof combustion chamber, dual overhead camshafts, and a centrally located spark plug (disabled for HCCI tests). At each experimental test point a total of 300 consecutive engine cycles are recorded for steady input conditions. The range of engine operating conditions are shown in Table 2, with a total of 13 test cases for this study. Cylinder pressure is measured with a Kistler ThermoCOMP model 6043A60 piezoelectric pressure transducer measured at 0.1 CAD resolution from a BEI optical encoder. Crank angle based parameters are recorded with an MTS Powertrain Baseline CAS system. The pressure signal is also sent to National Instruments LabVIEW for knock detection. Other engine operating parameters are measured at 10Hz with an MTS Power-train Baseline DAC and averaged over the entire test. Intake manifold air temperature, oil temperature, and coolant temperature are measured with K-type thermocouples. Equivalence ratio is measured with an ECM AFRecorder 1200 wideband oxygen sensor. The engine is equipped with two separate fuel systems, one supplying n-heptane and the other iso-octane to the two port fuel injectors. As the primary reference fuel (PRF) octane number (ON) is defined as the volume percentage of iso-octane in an iso-octane/n-heptane mixture, the PRF ON can be changed online by changing the ratio of the pulse widths of the two injectors. Since the auto-ignition quality of the mixture is changed with changes in PRF blend [17], the PRF ON can be used to control the amount of knock. A dSpace microautobox modulates the injector pulse widths to control both fuel energy and PRF ON.

DATA COLLECTION

The test procedure is to first warm up the engine in SI mode, and then make the transition to HCCI mode by increasing the intake manifold pressure with the supercharger, removing spark, reducing octane number, and increasing intake temperature with a heating element. Test conditions are performed at a steady engine speed, intake manifold pressure and temperature. A range of data is collected with varying degrees of knock. Comparing two cases, a high knock (Case A) and low knock case (Case B),

Table 1. Configuration of the Ricardo single-cylinder engine

Parameters	Values
Bore × stroke [mm]	80 × 88.9
Compression Ratio	10
Displacement [L]	0.447
Valves	4
IVC [aBDC]	22
EVO [aBDC]	11

Table 2. Engine operating conditions

Operating Condition	Values
Engine speed [rpm]	900 - 1150
Intake Temperature [deg C]	60
Intake Pressure [kPa]	100-120
Equivalence Ratio	0.32-0.36
EGR [percent]	0
coolant temperature [deg C]	60-70

is found to provide insight. The two cases are run at the same operating conditions except Case A has more fuel injected. Figure 1 shows one typical cylinder cycle for Case A and Case B as a function of crank angle in degrees after top dead center (TDC). The pressure trace for Case A shows a significant high frequency pressure oscillation starting near the location of peak pressure. These high frequency pressure waves are denoted as knock and are not desirable as they can damage the engine. It should be noted that the location of the pressure transducer effects the intensity of knock detected and that the location of the sensor was dictated by engine geometry. Thus the actual pressure oscillation intensity may be larger than that detected. The high frequency oscillations are found from $0 \leq CAD \leq 50$. This range is part of the expansion phase which is taken from TDC to the exhaust valve opening.

KNOCK QUANTIFICATION

The frequency of the pressure oscillations in the combustion chamber induced by the nonuniform combustion can be predicted using acoustic theory, as originally presented in [18]. There is generally one dominant mode of oscillations present in the pressure oscillations which tends to be the first circumferential mode for most engines. The first circumferential mode is the lowest frequency shown in Figure 2. The expected frequency of this mode is calculated by:

$$f_{m,n} = \frac{c\rho_{m,n}}{\pi b} \quad (1)$$

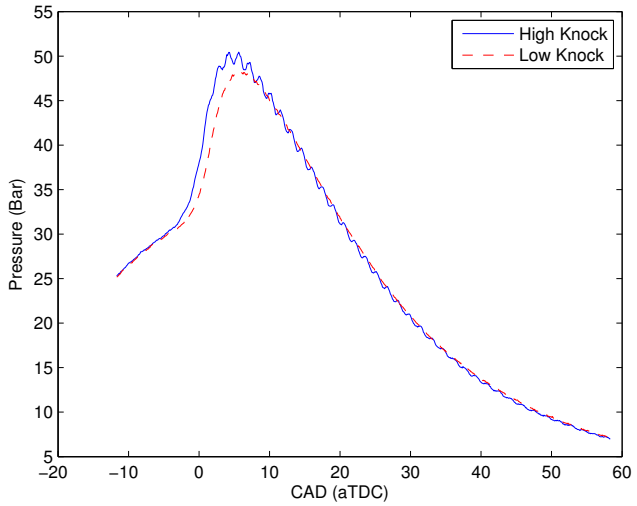

Figure 1. Pressure signal for: Case A - high knock; Case B: low knock

where $f_{m,n}$ is the Pressure oscillation frequency in Hz, m is the order of the circumferential mode, n is the order of the radial mode, c is the speed of sound in m/s, $\rho_{m,n}$ is a factor describing the mode, and b is the cylinder bore diameter in m. The speed of sound is approximated as 950 m/s [19]. The modes predicted for this engine from the acoustic theory are estimated for comparison with Fourier techniques as well as with wavelet methods. For the given engine bore size of 97 mm, the oscillation frequencies, in kHz, for the various modes are shown in Table 2. A more detailed analysis of the modes of oscillation can be found with a geometry describing a more modern pent roof style 4 valve combustion chamber [20]. In this work, the dominant mode is found to be the first circumferential mode, $\rho_{1,0}$ with $f_{1,0} = 5.7$ kHz, throughout the majority of the expansion stroke.

m,n	1,0	2,0	0,1	3,0	1,1
$p_{m,n}$	1.84	3.05	3.83	4.20	5.33
$f_{m,n}$ (Khz)	5.7	9.5	12	13	17

Figure 2. Frequency modes in a cylinder

From Fourier analysis, the estimated Power Spectral Density (PSD) of the pressure signal, for high knock (Case A) and low knock (Case B) cases, are shown in Figures 3 and 4, respectively. The PSD for the two plots has a frequency resolution of 58 Hz and uses Welch's averaged, modified periodogram method.

Comparing the peak of the PSD with the modal frequencies predicted by the acoustic analysis in Table 2, it can be seen that the peak at 5 kHz coincides with the first circumferential mode, $f_{1,0} = 5.7$ kHz. This frequency is apparent in both high knock (Figure 3) and low knock (Figure 4) cases. Zooming in

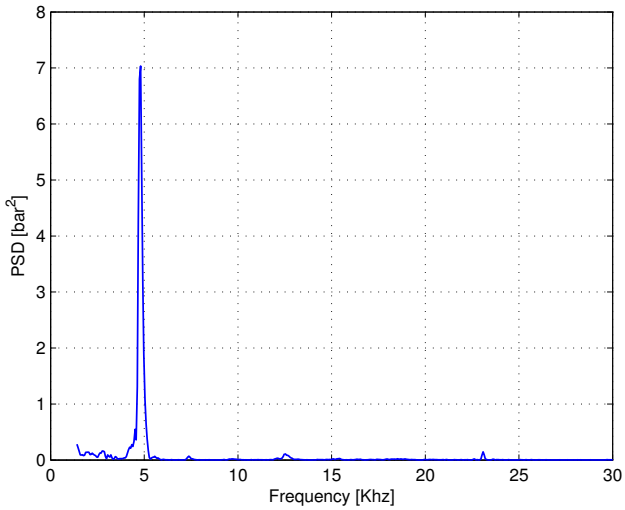

Figure 3. PSD of cylinder pressure for a high knock case (Case A) for a single cycle

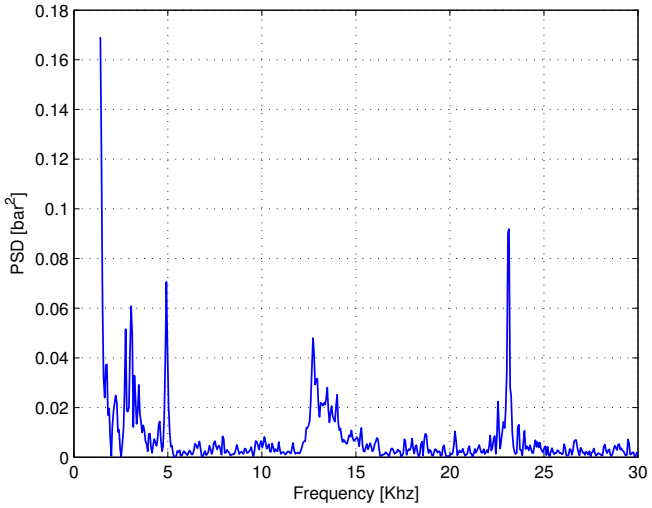

Figure 4. PSD of a low knock case (Case B) for a single cycle

on the high knock case in Figure 5, in the range of 10 kHz-15 kHz, smaller peaks at 9.5 kHz, 12 kHz, and 12.5 kHz are apparent. These correspond to $f_{2,0} = 9.5$ kHz, $f_{0,1} = 12$ kHz, and $f_{3,0} = 13$ kHz frequency modes.

The difference between the calculated frequency modes and the observed frequencies is attributed to the combustion chamber geometry, the speed of sound difference, and potential axial vibration modes. For the low knock case, which has lower peak amplitudes, an oscillation frequency of 22 kHz is prominent perhaps due to the resonance frequency of the engine [21]. However, the magnitude of this peak is almost a factor of 100 lower than the main peak in Case A. The frequencies that are present in the PSD are not distinct but rather are "smeared" over a range of frequencies. During the power stroke both

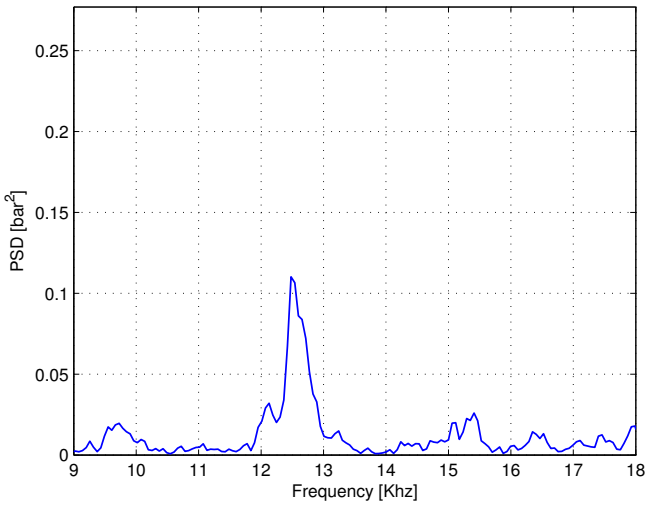

Figure 5. PSD of the high knock case for frequency range of 9 kHz to 20 kHz

the gas temperature and chamber volume change causing a decaying mode frequency. Thus the knock frequency decreases with time making PSD estimation of the knock intensity more difficult. However, the prominent PSD amplitude of the first circumferential mode during engine knock makes it the best choice as a knock detection measure [19].

1 Knock Benchmark - Root Mean Squared of Pressure

As the pressure transducer is the most direct measurement of the pressure oscillations induced by knock, this transducer is used for knock measurement. A commonly used benchmark method for knock identification is the value of the root mean square power (RMS) of the pressure signal, in the frequency range of the knocking, typically 4-7 kHz [19]. The value of P_{RMS} is defined by

$$P_{RMS} = (\frac{1}{N}[\hat{p} \cdot \hat{p}])^{\frac{1}{2}} \quad (2)$$

Here the value of $\hat{p}$ has been determined by bandpass filtering of the pressure trace using a 10th order Butterworth filter, with a pass band of 3-10 kHz and N is the number of pressure points collected (N=1800 here). The knock index, K_{PSD}, is determined from the PSD using an averaging method around the first

and second mode of the knock frequencies (3 kHz to 10 kHz) as

$$K_{PSD} = \left(\frac{\sum_{i=L}^{H} PSD}{H-L} \right)^{\frac{1}{2}} \quad (3)$$

Where L and H are the bins corresponding to 3 and 10 kHz, respectively. Figure 6 shows the relationship between the P_{RMS} and K_{PSD} for 300 engine cycles of high knock (case A) and 300 cycles low knock (case B). It can be seen that there is an overlap of the knock index from the high knock case to the low knock case which indicates that there is inherent variability in the amount knock from cycle to cycle [22].

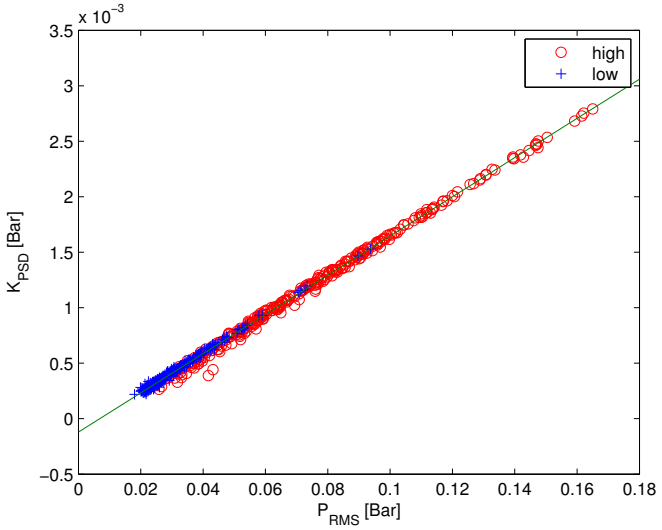

Figure 6. Comparison of pressure PSD to benchmark for both high and low knock case

WAVELET ANALYSIS

2 CONTINUOUS WAVELET TRANSFORM

The Continuous Wavelet Transform (CWT), unlike the Fourier transform, is a transformation with a basis function that is non-periodic and localized in time. To perform the wavelet transform, the basis function is shifted in time and is scaled(stretched/compressed), and correlated with the signal. By cross-correlating the basis function of different time shifts and scales with the signal, the wavelet coefficients indicate the frequency spectrum. For a continuous signal both the time shift and scale can be varied continuously. In practice, using sampled data, the time shift can only be reduced to the sample rate and a finite number of scales (frequency equivalent) are chosen to approximate a continuous wavelet transform (CWT). The relationship between scale, s, and frequency, F_{scaled}, is given by

$$F_{scaled} = \frac{F_{center}}{s\Delta} \quad (4)$$

where F_{center} is the center frequency of the wavelet chosen, and $\triangle$ is the sampling frequency of the signal.

The CWT with a scale range of 0.5 to 21.5, converted to pseudo-frequency for high knock and low knock can be seen in Figures 7 and 8, respectively. The resulting CWT coefficients are displayed as blue for low correlation or red for the highest correlation to the chosen wavelet. Using the complex Morlet wavelet it can be seen that in the heavy knock case there is a range of frequencies identified about the combustion event. These frequencies range from 4.5 kHz to 9 kHz, corresponding to the expected knock frequency, with the peak intensity at 5.7 Khz. If the CWT wavelet coefficients for the no knock case are plotted on the same scale, they are too small to be seen. Instead, in Figure 8, the scale magnitude is reduced by a factor of 10 compared to Figure 7 and shows that these frequencies are negligible. The peaks that can be seen at -90 and -10 CAD are most likely artifacts of the signal processing technique. Thus the CWT method can detect knock and can quantify it by the magnitude of the wavelet coefficients. However, the CWT method is computationally intensive and thus is suitable for off-line analysis. For real time knock detection the discrete wavelet transform is used as it can be efficiently implemented as a filter bank.

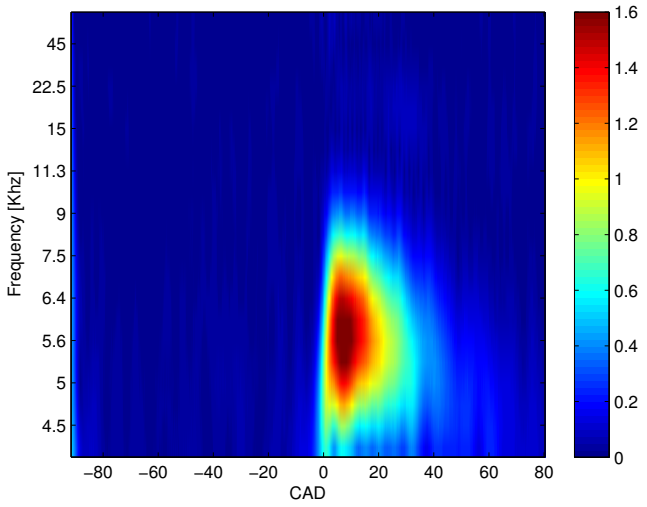

Figure 7. CWT Morlet coefficients for heavy knock case

3 DISCRETE WAVELET TRANSFORM

The Discrete Wavelet Transform (DWT), with a Daubechies-8 (16 coeffients) basis function, is used to analyze the knock signal. A three level filter bank is created where

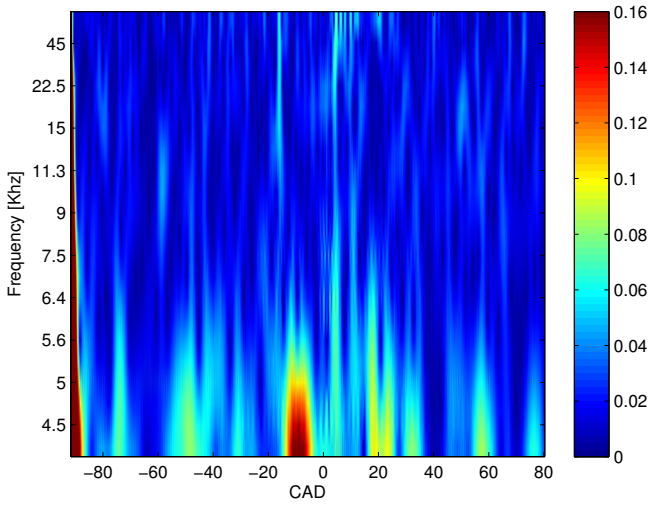

Figure 8. CWT Morlet coefficients for low knock case

the signal is decomposed into the detail (high frequency) and approximation (low frequency) coefficients. The third level decomposition is shown in Figure 9 with CAD on the X-axis and frequency ranges on the Y-axis.

This format is similar to the CWT plots for both high and low knock cases. The frequency range of 3.57 to 7 kHz is the knock frequency range and is thus the important range to compare for Case A and Case B. It can be seen that the knock frequency of 5 kHz is seen in the DWT plot for the high knock case but is absent in the low knock case. Thus the DWT contains the important knock information, similar to the CWT. The maximum of the signal in the 3.75 to 7.5 kHz range is taken to be the knock index and is used for real time knock detection. The knock index is recorded along with the pressure trace in order to compare the DWT detection method. Figure 10 compares the real time DWT detection method to the P_{RMS} method for each of the 300 engine cycles of both high (case A) and low knock (case B) and a linear correlation is seen. However, the correlation contains more scatter than the P_{PSD} method. This is mostly due to the wavelet chosen and its correlation to the shape of the knock oscillations. Using a wavelet based on the shape of the pressure oscillation itself may offer better results [23]. Thus a potential drawback of using the DWT method with a simple wavelet, such as the Daubechies, is the difficulty in controlling a system with high measurement error. The DWT method is implemented as a filter bank which takes 2 ms to calculate (in LabVIEW on a 2.7 GHz processor). With the engine running at 1000 RPM the cycle time is 120 ms so the DWT method can easily be implemented in a real time knock control scheme.

KNOCK CONTROL

Knock is induced into the system by increasing the fuel injection pulse width to increase the injected fuel energy by 0.035KJ, from 0.6611KJ (case A) to 0.6961KJ (case B), at an operating point near knock. The engine speed is 1000 RPM and

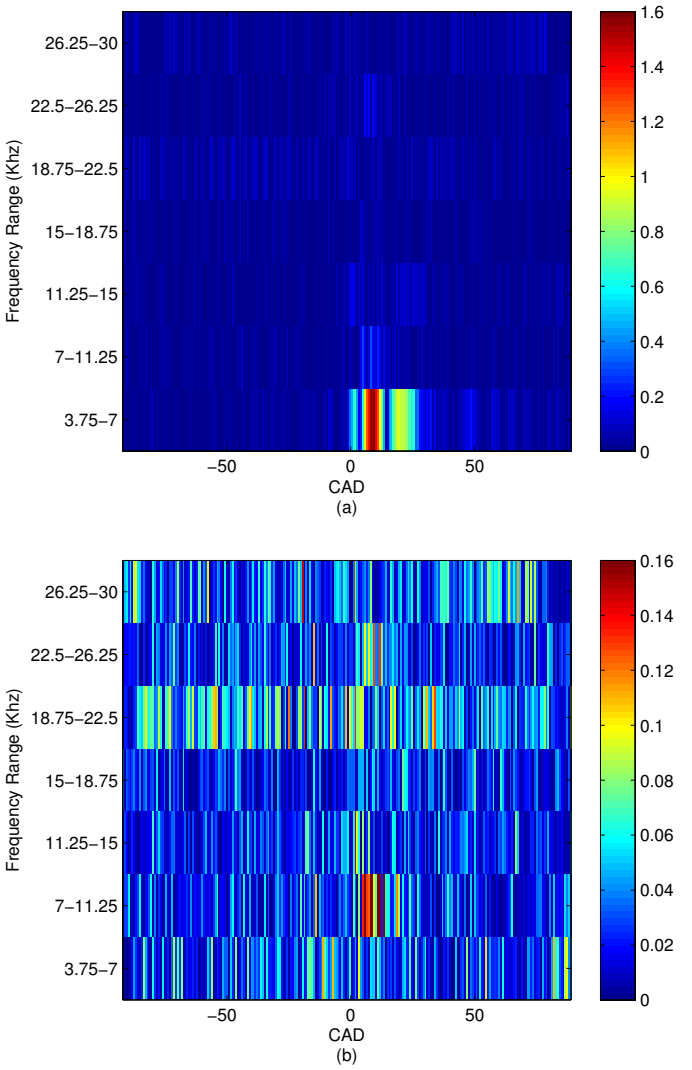

Figure 9. DWT colored coefficients for (a) high and (b) low knock cases

other conditions are as specified in Table 2. The step in fuel energy is defined to occur from cycle 0 to cycle 1. In Figure 11 the fuel energy is stepped up while keeping the octane number constant. The resulting increase of knock without any control, with a five cycle moving average due to the high cyclic variation, is shown in Figure 11.

To control the knock level despite a step in fuel energy, these three controllers are examined: Feed-Forward (FF), Proportional Integral (PI), and and PI+FF. A block diagram of the overall control system is shown in Figure 12 with switches turning the individual controllers on or off. The control actuation is the fuel octane number which is changed using dual injectors of n-heptane and iso-octane. The fuel octane has been shown to directly affect knock [24]. The fuel injection event is performed while the intake valve is closed (TDC = 0 degrees). This was needed in order to allow the fuel to evaporate. The desired knock value from the DWT method was set heuristically to 0.18 Bar based on auditory and visual information during testing.

Feed-Forward control is shown in Figure 13. The step dis-

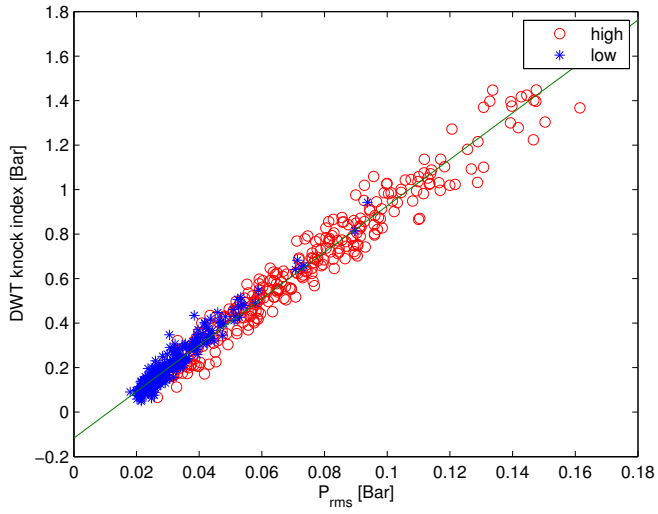

Figure 10. DWT correlation to Benchmark

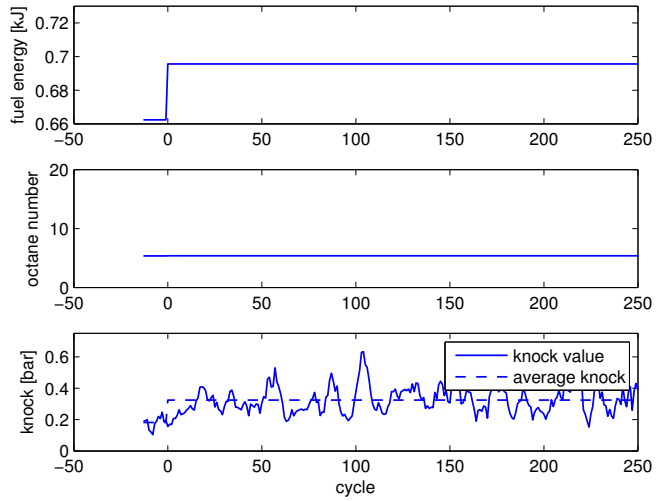

Figure 11. Knock level response to step in fuel energy - no control

turbance in fuel energy is initiated at cycle zero and it can be seen that the fuel octane is commanded to jump immediately by 9 PRF ON. The jump was chosen by manual tuning. Comparing Figure 11 and 13 shows that the fluctuations in knock are much better than the no control case but are still higher in average and fluctuate after the fuel jump.

Figure 14 illustrates the resulting knock level with PI control, with the dashed line indicating the desired knock level for the PI controller. The gains for the controller were tuned by first increasing the proportional gain until oscillations in the knock level could be seen. The proportional gain was then reduced and the integral gain was increased until the desired knock level response was achieved. The final gains for the proportional and integral gains are 0.00011 and 0.00002 respectively. It takes approximately 25 cycles for the octane number to reach the new steady state.

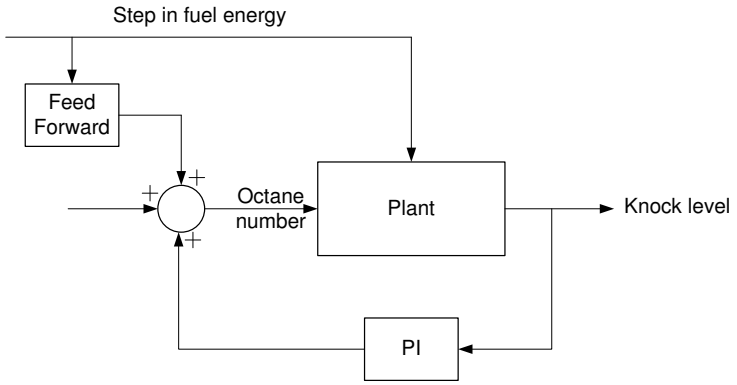

Figure 12. Block diagram of the FF and PI controllers

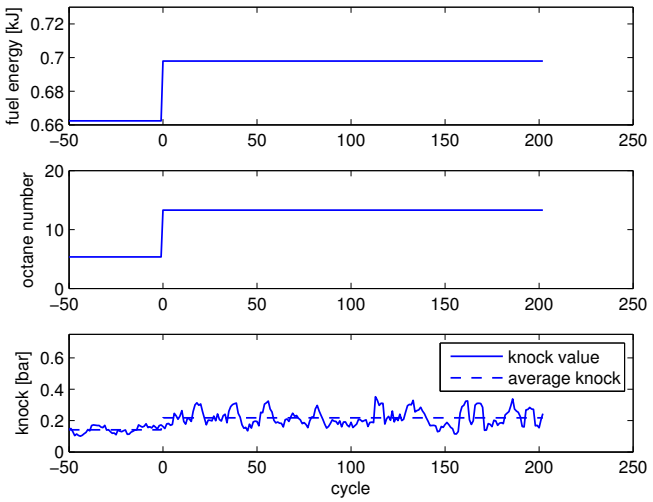

Figure 13. Knock level response to step in fuel energy - FF control

Finally, Feed-Forward is combined with PI control and the resulting knock response is shown in Figure 15. The octane command jumps immediately in Figure 15 due to the FF command and the resulting knock level appears to have less fluctuations when compared to Figure 13. Table 3 shows a comparison of knock level and standard deviation for the different cases. Table 3 first shows the normalized standard deviation of the four cases where σ_1 is the standard deviation of the knock level before the fuel jump and σ_2 is the standard deviation of the knock level after the fuel jump. In the base case and in the Feed-Forward, the volatility of the knock value increase by at least 100 percent. With the PI controller, the standard deviation increases by 11 percent, and the addition of Feed-Forward lowers that deviation to 6 percent.

The normalized deviation from the desired knock value is also tabulated in Table 3. κ_1 is the deviation from the knock level set-point before the fuel jump and κ_2 is the deviation from the knock set-point after the fuel jump normalized around the set point of 0.18 Bar. The ratio of κ_2/κ_1 illustrates how the average knock value changed from the desired 0.18 Bar set point.

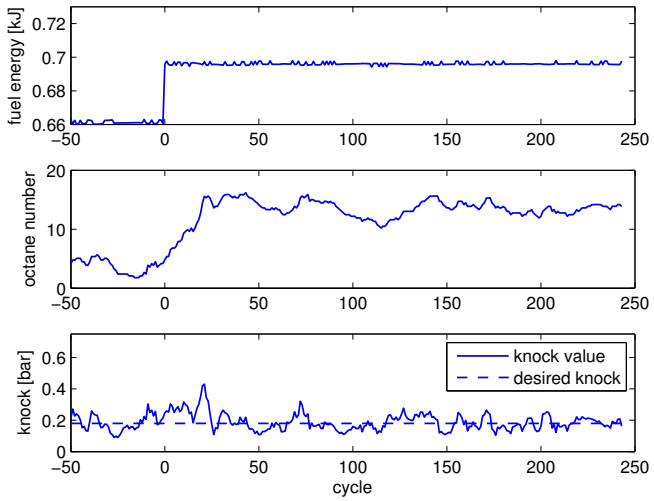

Figure 14. Knock level response to a step in fuel energy - PI control

For both the baseline case as well as the Feed-Forward case, the knock level increases 80 percent and 50 percent respectively. By using PI controller (with or without Feed-Forward), the knock level is within 3 percent of the desired value. When the knock level in Figure 15 is compared to Figure 14, the addition of FF seems to reduce the knock fluctuation right after the step in fuel energy.

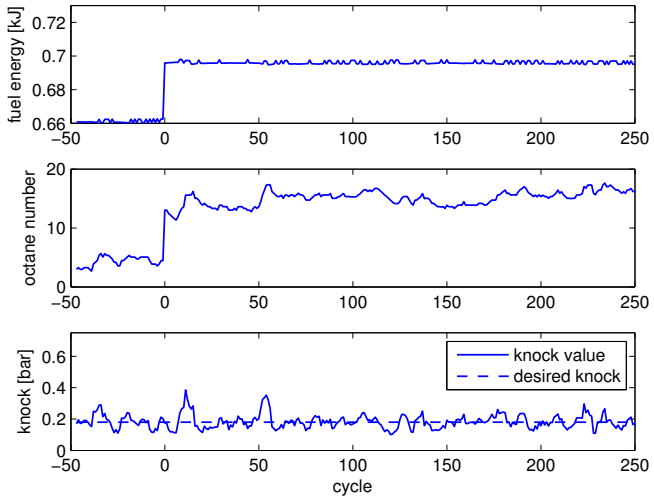

Figure 15. Knock level response to a step in fuel energy - PI+FF control

CONCLUSIONS

Due to the simplicity and time resolution, time-frequency based methods such as the wavelet transform are better suited than the Fourier transform method for knock detection. The discrete wavelet transform is chosen for real time knock detection in HCCI since the processing consists of passing the signal through filter coefficients making it computationally efficient. The method of determining knock through DWT was compared to the benchmark method and proved to be linearly correlated. The knock signal was then used to compare three control schemes to the baseline case of no knock: PI, Feed-Forward, and PI with Feed-Forward. Fuel Energy was used to initiate knock and octane number was used to control the knock level. The PI control significantly reduced the variance as well as keeping the knock level close to the desired set-point. The PI with Feed-forward could marginally improve the performance of the controller.

Table 3. Comparison of control schemes to no control case

	No Control	FF	PI	PI and FF
σ_2/σ_1	2.17	2.40	1.11	1.06
κ_2/κ_1	1.79	1.54	1.03	0.98

REFERENCES

[1] J. M. Grenda. Numerical modelling of charge stratification for the combustion control of HCCI engines. *SAE paper No. 2005-01-3722*, October 2005.

[2] P. G. Aleiferis, A. G. Charalambides, Y. Hardalupas, A. M. K. P. Taylor, and Y. Urata. Modelling and experiments of HCCI engine combustion with charge stratification and internal EGR. *SAE Paper No. 2005-01-3725*, 2005.

[3] M. Sjberg and J. Dec. Smoothing HCCI heat-release rates using partial fuel stratification with two-stage ignition fuels. *SAE Paper No. 2006-01-0629*, 2006.

[4] A. W. Berntsson and I. Denbratt. HCCI combustion using charge stratification for combustion control. *SAE Paper No. 2007-01-0210*, 2007.

[5] T. Tsurushima, E. Kunishima, Y. Asaumi, Y. Aoyagi, and Y. Enomoto. The effect of knock on heat loss in homogeneous charge compression ignition engines. *SAE Paper No. 2002-01-0108*, 2002.

[6] A. R. Ashrafzadeh, A. M. Makki, and H. Servati. Quantitative analysis of knock sensor utilizing real-time discrete Fourier Transform (DTDFT). *SAE Paper No. 1991-25-0100*, 1991.

[7] S. Vulli, J. F. Dunne, R. Potenza, D. Richardson, and P. King. Time-frequency analysis of single-point engine-block vibration measurements for multiple excitation-event identification. *Journal of Sound and Vibration*, 321:1129–1143, 2008.

[8] R. C. Geradin, B. N. Huallpa, M. F. Alves, and J. R. Fran Arruda. Analysis of spark ignition engine knock signals using Fourier and discrete wavelet transform. *SAE Paper No. 2009-36-0312*, 2009.

[9] J Chang, M Kim, and K Min. Detection of misfire and knock in spark ignition engines by wavelet transform of engine block vibration signals. *Measurement Science and*

Technology, 13(7):1108–1114, Jul. 2002.

[10] J.M. Borg, K.C. Cheok, G. Saikalis, and S. Oho. Wavelet-based knock detection with fuzzy logic. *CIMSA. 2005 IEEE International Conference on Computational Intelligence for Measurement Systems and Applications, 2005*, pages 26 – 31, Jul. 2005.

[11] Z. Zhang and E. Tomita. A new diagnostic method of knocking in a spark-ignition engine using the wavelet transform. *SAE Paper No. 2000-01-1801*, 2000.

[12] J. Souder, J. Mack, J. Hendrick, and R. Dibble. Microphones and knock sensors for feedback control of HCCI engines. *ASME Internal Combustion Engine Division*, 2004.

[13] B. Yunlong, W. Zhi, and W. Jianxin. Knocking suppression using stratified stoichiometric mixture in a disi engine. *SAE Paper No. 2010-01-0597*, 2010.

[14] J. C. Peyton Jones, J. Frey, K. R. Muske, and D. J. Scholl. A cumulative-summation-based stochastic knock controller. *Proceedings of the Instituion of Mechanical Engineers Part D-Journal of Automobile Engineering*, 224(D7):969–983, 2010.

[15] X. Lu, D. Han, and Z. Huang. Fuel design and management for the control of advanced compression-ignition combustion modes. *Progress in Energy and Combustion Science (in press)*, 2011.

[16] T. Lakshmanan and G. Nagarajan. Experimental investigation on dual fuel operation of acetylene in a di diesel engine. *Experimental investigation on dual fuel operation of acetylene in a DI diesel engine*, 91:496–503, 2010.

[17] M. J. Atkins and C. R. Koch. The effect of fuel octane and diluent on HCCI combustion. *Proc. IMechE, Part D*, 219:665 – 675, 2005.

[18] C. S. Draper. The physical effects of detonation in a closed cylindrical chamber. Technical Report 493, National Advisory Committee for Aeronautics, 1933.

[19] J. M. Borg, G. Saikalis, S. Oho, and K. C. Cheok. Knock signal analysis using the discrete wavelet transform. *SAE Paper No. 2006-01-0226*, 2006.

[20] D.Schroll, C. Davis, S. Russ, and T. Barash. The volume acoustic modes of spark ignited inernal combustion chambers. *SAE Paper No. 980893*, 1998.

[21] C. J. Polonowski, V. K. Mathur, J. D. Naber, and J. R. Blough. Accelerometer based sensing of combustion in a high speed HPCR diesel engine. *SAE Paper No. 2007-01-0972*, 2007.

[22] A. Vressner, A. Lundin, M. Christensen, and P. T. B. Johansson. Pressure oscillations during rapid HCCI combustion. *SAE Paper No. 2003-01-3217*, 2003.

[23] Z. Zhang and E. Tomita. Diagnostic of knocking by wavelet transform method utilizing real signal as mother wavelet. *SAE Paper No. 2001-01-3546*, 2001.

[24] A. Audet. *Closed Loop Control of HCCI using Camshaft Phasing and Dual Fuel*. Msc. Thesis, 2008.